Cement and Concrete Research 42 (2012) 928–936

Contents lists available at SciVerse ScienceDirect

Cement and Concrete Research

journal homepage: http://ees.elsevier.com/CEMCON/default.asp

E-modulus evolution and its relation to solids formation of pastes from commercial cements

Lino Maia [a,b,*], Miguel Azenha [c], Mette Geiker [d,e], Joaquim Figueiras [a]

[a] LABEST – Laboratory for the Concrete Technology and Structural Behaviour, Faculdade de Engenharia, Universidade do Porto, Rua Dr. Roberto Frias, 4200-465 Porto, Portugal
[b] Centro de Ciências Exatas e da Engenharia, Universidade da Madeira, Campus Universitário da Penteada, 9020-105 Funchal, Portugal
[c] ISISE – Institute for Sustainability and Innovation in Structural Engineering, Universidade do Minho, Escola de Engenharia, Campus de Azurém, 4800-058 Guimarães, Portugal
[d] DTU – Department of Civil Engineering, Technical University of Denmark, Brovej, Building 118, DK-2800 Kgs. Lyngby, Denmark
[e] NTNU – Department of Structural Engineering, Norwegian University of Science and Technology, Rich. Birkelandsvei 1A, 7491 Trondheim, Norway

ARTICLE INFO

Article history:
Received 12 May 2011
Accepted 16 March 2012

Keywords:
Hydration (A)
Elastic moduli (C)
Cement paste (D)
Resonant frequency
Limestone filler (D)

ABSTRACT

Models for early age E-modulus evolution of cement pastes are available in the literature, but their validation is limited. This paper provides correlated measurements of early age evolution of E-modulus and hydration of pastes from five commercial cements differing in limestone content. A recently developed methodology allowed continuous monitoring of E-modulus from the time of casting. The methodology is a variant of classic resonant frequency methods, which are based on determination of the first resonant frequency of a composite beam containing the material. The hydration kinetics — and thus the rate of formation of solids — was determined using chemical shrinkage measurements. For the cements studied similar relationships between E-modulus and chemical shrinkage were observed for comparable water-to-binder ratio. For commercial cements it is suggested to model the E-modulus evolution based on the amount of binder reacted, instead of the degree of hydration.

© 2012 Elsevier Ltd. All rights reserved.

1. Introduction

Early age cracking of cement-based materials is a major problem associated with cement hydration. The cracking is caused by the development of stresses due to restrained autogenous and thermal deformations developed after the transition from fluid-to-solid [1–3]. The stress development is directly related to the E-modulus, which evolves faster than the strength at early ages [4]. Therefore, among others, knowledge on the E-modulus evolution is central for accurate sustained stress predictions and corresponding cracking risk evaluation.

The E-modulus evolution of cement-based materials is related to the growth of solid volume and the degree of connectivity of the solids. The E-modulus evolution is therefore usually described as a function of the degree of hydration. Several authors [5–11] have proposed microstructural models to predict and explain the E-modulus and the Poisson's ratio evolutions as a function of the degree of hydration. Mostly, for prediction of E-modulus, models use a lattice-based approach [12], i.e. it is assumed that a specific volume of study is represented by a set of voxels, each of which may contain: (i) empty or water filled pore, (ii) anhydrous cement or (iii) hydrated cement. The elastic properties are thus calculated based on the elastic properties [13–15] of each individual voxel and its degree of interconnectivity. The predictions are affected by several modelling parameters [5], such as: the resolution, the mesh type or isolated clusters. Even though these issues may have a high impact on the accuracy of the E-modulus prediction, the referred models provide insights for the explanation of the influence of the constituent materials and mix compositions on the evolution of elastic properties (for instance: the water-to-binder ratio and the particle size distribution of the binder).

For assessment of models and modelling parameters, authors [5–11] faced validation problems because it is difficult to measure the E-modulus, especially at very early ages while the material's strength and stiffness is still small. In fact, up to this date, only few experimental studies of E-modulus evolution of cement-based pastes can be found in the literature [5,7,16–18]. Among them, solely Boumiz [16] reported continuous E-modulus measurements as a function of the degree of hydration. Consequently, his findings are being used as the main experimental source for model validation of the numerical methods mentioned above.

When using Boumiz's results [16] for model validation, one should be aware that: the studies were carried out on pastes made from C_3S and white Portland cement (which are different from the most commonly used commercial cements owing to the existence of different clinker phases and the incorporation of additions); and that the elastic properties were estimated using ultrasonic compressional and shear waves (which might lead to values rather close to the dynamic E-modulus [19]). Besides, if researchers intend to carry out ultrasonic tests to validate their models, they have to face problems related to: (i) material inhomogeneity because compressional waves do not

* Corresponding author. Tel.: +351 966096541; fax: +351 225081835.
E-mail addresses: lino.maia@fe.up.pt (L. Maia), miguel.azenha@civil.uminho.pt (M. Azenha), mge@byg.dtu.dk, mette.geiker@ntnu.no (M. Geiker), jafig@fe.up.pt (J. Figueiras).

0008-8846/$ – see front matter © 2012 Elsevier Ltd. All rights reserved.
doi:10.1016/j.cemconres.2012.03.013

propagate properly through plastic pastes not de-aired [20], and (ii) shear waves do not propagate in fluid mediums and consequently the velocity of the first shear wave can only be measured after setting has already occurred [16].

Paste E-modulus can be continuously measured from the time of casting by the 'Elasticity Modulus Monitoring through Ambient Response Method' (EMM-ARM) [21]. This method, which was initially developed for concrete by Azenha et al. [22], is based on measurement of the natural frequency of an isostatic composite beam filled with the material to be tested. The EMM-ARM was used by Maia et al. [18] to study the influence of several additions (limestone, fly ash, silica fume and metakaolin) on the E-modulus evolution of cementitious pastes. However, the determination of E-modulus evolution through the EMM-ARM lacks of comparison to other experimental techniques. Furthermore, the E-modulus values reported in Ref. [18] are much lower than those reported by Boumiz [16], obtained through ultrasonic testing.

The overall purpose of this paper is to contribute to the description and understanding of the early age E-modulus evolution in pastes made from commercial cements. The E-modulus evolution was determined by the EMM-ARM. At first, continuous measurements of E-modulus obtained using the EMM-ARM are compared to results from quasi-static tests in order to check the suitability of the EMM-ARM for measurement of E-modulus of cement pastes (and thus for validation of micromechanical models). The E-modulus evolution is compared to the hydration kinetics (and thus the formation of solids), of pastes having different w/c ratios and/or limestone filler content. The hydration kinetics was assessed by chemical shrinkage. The effect of limestone filler incorporated in the commercial cements is evaluated and the applicability of a corrected w/b ratio (according to the amount of limestone filler that will not react [23]) to describe solid formation is demonstrated.

2. Materials and methods

The E-modulus evolution was measured for seven pastes using the EMM-ARM and hydration kinetics was determined from chemical shrinkage measurements. A two stage experimental program was undertaken: (i) pastes with w/c 0.40, 0.45 and 0.50 from the same cement; and (ii) pastes with w/c = 0.45 from four other cements incorporating different limestone filler contents. The percolation theory was applied on E-modulus values in order to detect the transition from fluid-to-solid. Quasi-static tests and ultrasonic compressional waves were carried out for some pastes in order to allow comparison between methods.

2.1. Materials, mixing, casting and curing

All cement pastes were prepared from commercial cements that are currently available on the Portuguese market. The cements CEM I 52.5R, CEM I 42.5R, CEM II/A-L 42.5R, CEM II/B-L 32.5N and CEM II/B-L 32.5R (white), according to EN 197-1 [24], were used. Table 1 presents their compositions and properties (based on information provided by the cement producer — average analyses of the month from which the cement used was produced); the Bogue composition was calculated according to Ref. [25] and the maximum chemical shrinkage according to Ref. [26].

The cements were mixed with distilled water to give w/c = 0.45 as a compromise between limited bleeding [27] and sufficiently high w/c ratio to ensure adequate connectivity in the pore structure to facilitate chemical shrinkage measurements [28]. Pastes with w/c = 0.40 and w/c = 0.50 were also prepared from cement CEM I 42.5R. All cement pastes were made twice: (i) once for the EMM-ARM using 320 g of cement, and (ii) once for the chemical shrinkage tests using 160 g of cement.

All tests were performed at 20 °C and carried out for at least 168 h. The temperature inside the samples for the EMM-ARM was measured; the maximum temperature increase in regard to room temperature was lower than 0.5 °C and temperature effects were therefore neglected.

Table 1
Components, Bogue composition and other cement characteristics. Percentages are with respect to mass; V_{pot} is the calculated chemical shrinkage at full hydration [26].

Cement	CEM I 52.5R	CEM I 42.5R	CEM II/A-L 42.5R	CEM II/B-L 32.5N	CEM II/B-L 32.5R white
Loss of ignition [%]	1.6	3	5.3	10.33	12.45
Insoluble residue [%]	0.9	1.1	1	2.5	0.42
Silicon Oxide [%]	20.16	19.82	18.56	18.02	17.6
Aluminate Oxide [%]	4.35	4.22	4.16	3.86	2.38
Iron Oxide [%]	3.48	3.4	3.22	2.52	0.17
Calcium Oxide [%]	62.97	62.66	62.02	59.7	64.58
Magnesium oxide [%]	2.33	2.21	2.09	1.79	0.5
Sulphates [%]	3.4	3.47	3.35	2.61	2.48
Potassium oxide [%]	–	–	–	–	–
Sodium oxide [%]	–	–	–	–	–
Chlorides [%]	0.03	0.03	0.03	0.0162	0.0195
Free lime [%]	1.37	1.28	1.29	0.88	3.3
N/D (no dosed) [%]	1.75	1.52	1.45	–	–
C_3S [%]	54	50	52	35	57
C_2S [%]	17	19	14	26	8
C_3A [%]	6	5	6	6	6
C_4AF [%]	11	10	10	8	0.5
Limestone filler [%]	0.0	4.5	9.2	22.7	26.2
Gypsum [%]	6.7	5.2	5.6	4.2	4.1
Blaine [cm^2/g]	4914	4112	4494	4433	5019
Specific gravity [g/cm^3]	3.14	3.12	3.09	3.06	2.98
V_{pot} [ml/g of cement]	0.0626	0.0609	0.0585	0.0534	0.0506

Mixing of samples for determination of E-modulus by the EMM-ARM and of samples for measurement of chemical shrinkage was performed in plastic containers using a mixer with a vertical paddle according to the following procedure: (i) add water to powders (instant defined as 't = 0'); (ii) start mixing at 500 rpm and mix for 3 min; (iii) stop mixing for 2 min; (iv) resume mixing at 2000 rpm for 2 min. All samples for E-modulus measurement were cured sealed.

Samples for E-modulus measurements by quasi-static tests, were prepared from pastes of the following compositions: (i) CEM I 42.5R — w/c = 0.40, (ii) CEM I 52.5R — w/c = 0.45, and (iii) CEM II/B-L 32.5R (white) — w/c = 0.45 (paste compositions were chosen to avoid bleeding problems [27]). Pastes for quasi-static test were prepared following a procedure close to the norm EN 196-1 [29], with the following minor changes: (i) batches were prepared using 2200 g of cement; (ii) mixing was started and continued for 3 min at 'low speed' (defined in Ref. [29]); (iii) mixing was then stopped during 2 min; (iv) mixing was resumed for 2 min at 'high speed' (defined in Ref. [29]); (v) samples were kept moulded inside a climatic chamber at T = 20 °C and RH = 50% up to the onset of testing. However, it was noted that owing to sample dimensions ($4 \times 4 \times 16\ cm^3$), the temperature inside the samples increased by several degrees Celsius (the maximum was 8 °C for the paste CEM I 52.5R). Therefore, the temperature was automatically measured every minute approximately at the centre of samples in order to allow the applicability of maturity corrections. Such corrections, in this research paper, were performed by employing the expression B.10 in the Eurocode 2 [30]. For instance, at the age of 24 h the temperature adjusted ages were 28.7, 29.5 and 26.7 h and at the age of 168 h were 175.2, 179.15 and 174.6 h, for pastes made from CEM I 42.5R — w/c = 0.40, CEM I 52.5R – w/c = 0.45 and CEM II/B-L 32.5R (white) — w/c = 0.45, respectively.

2.1.1. Mix compositions

According to Lothenbach et al. [23], limestone filler in excess approximately 5% of the amount of cement can be considered inert. A more detailed explanation is given in Section 3.5.

In the present work, the cements CEM II/A-L 42.5R, CEM II/B-L 32.5N and CEM II/B-L 32.5R (white) contain more than 5% of limestone (see Table 1). The part of the cement that is able to react is given by Eq. (1):

$$b = (c - f)/0.95 \quad (1)$$

where b is the amount of binder, c is the amount of cement and f the amount of limestone filler. Note that the following terminology is used in this present paper:

- 'cement' (c) is all the material that is supplied by the cement producer (commercial cement), i.e. the total powder supplied inside a bag (clinker, gypsum, limestone filler and so on);
- 'limestone filler' (f) is the amount of filler per weight of cement, given by the cement producer — see Table 1;
- 'binder' (b) is the part of cement that is able to react, given by the Eq. (1);
- 'w/c' is the water-to-cement ratio on mass basis;
- '$(w/c)_v$' is the water-to-cement ratio on volume basis;
- 'w/b' is water-to-binder ratio on mass basis;
- '$(w/b)_v$' is water-to-binder ratio on volume basis;
- '$c_{v\%}$' and '$b_{v\%}$' are, in percentage, the initial volume of cement and volume of binder in the paste, respectively.

In order to take into account the combined effect of the w/c ratio and the presence of limestone filler, the w/b ratios were calculated, see Table 2. To calculate the $(w/b)_v$, at first, the specific gravity of the binder ρ_b was calculated by the Eq. (2).

$$\rho_b = \frac{b}{\frac{c}{\rho_c} - \frac{c-b}{\rho_f}} \quad (2)$$

where ρ_c is the specific mass of the cement (given in Table 1) and ρ_f is the specific gravity of the limestone filler (in this work $\rho_f = 2.70$ g/cm^3 was considered).

2.2. Measurement of the E-modulus using the EMM-ARM

Several tests can be used to assess the E-modulus evolution of concrete through compressive load cycles, and various standards deal with this issue: ASTM C 469 [31] and ISO 1920-10 [32], among others. However, owing to their basic concept, these tests require that the sample is demoulded before testing, thus implying that the material has already developed some resistance. For a thorough description of the E-modulus evolution since the fluid-to-solid transition, methods that allow measurements from the time when casting is finished (while the resistance is null) are required. The rheometric methods are appropriate to describe the E-modulus evolution before setting [17,20,33,34], but soon after the material becomes solid they cannot be applied. In contrast, when methods based on wave propagation are used, the evolution at very early ages is not so clear. Nonetheless, the latter methods have a high range of applicability, being able to provide continuous measurements both on fluid and on hardened materials [35–37]. In the last few years, the ultrasonic methods have been extensively applied [16,20,36–41] to assess cement-based elastic and mechanical properties. However, as reported in Section 1 the ultrasonic methods face problems at very early ages related to propagation into fluid mediums and mediums containing air voids [16,20].

The EMM-ARM method is a variant of the standard resonant frequency methods [42] for continuous evaluation of E-modulus evolution of concretes, which has recently been proposed by Azenha et al. [22]. Through the continuous monitoring of the evolution of resonant frequency of a composite beam, filled with the material to test, this method allows the continuous estimation of the evolving E-modulus since casting, without any human intervention throughout its course of evolution. Based on the confidence gained by the observed coherence in regard to the E-modulus evolution assessed through the EMM-ARM and estimated through compressive cyclic tests in concrete cylinders, a lighter device was also developed for the study of pastes [21]. The validation of the results of EMM-ARM devised for cement pastes has been made against the results obtained with P-wave propagation since very early ages, with good coherences being obtained [43]. In view of the ability of this method to provide continuous measurements of E-modulus immediately after casting and onwards, the research reported in this paper encompasses the use of the lighter device of the EMM-ARM devised for pastes.

A brief outline of the overall test principle for the study of pastes is presented herein (for detailed information, see [21,22,44]) and supported by the photo in Fig. 1 that depicts a sample during a test, and by the scheme in Fig. 2, where the data processing flowchart is shown. Firstly, the paste to be studied is cast inside an acrylic tube, which is used as a mould. Then, after closing both extremities, a connection fastening device is attached to one of them, and the entire system is fixed and clamped through it, ensuring the structural behaviour of a horizontal composite cantilever beam. An accelerometer (with mass of 0.7 g and a sensitivity of 10 mV/g — 'g' is here the acceleration due to gravity) is placed at the opposite extremity of the cantilever (the free end), in order to monitor accelerations in the vertical direction induced just by ambient excitation. This ambient excitation corresponds to the vibrations that naturally occur in the vicinity of the experiment (for instance: people talking/walking; machinery; vehicles passing nearby the building; room ventilation). In this experimental program, the ambient excitation level was increased by placing a fan blowing air to the test specimen. The experiment can start as soon as all the parts are correctly placed, which usually occurs within ~20 min after mixing the cementitious material. In regard to data processing, schematized in Fig. 2, a brief description of the overall set of operations conducted to obtain the E-modulus curve is presented. The measured accelerations are acquired in a 24-bit data logger at a frequency of 200 Hz, and divided in sets of 5 min, each of which is treated according to the Welch procedure [45]. As a result, it is possible to obtain an averaged power spectrum of the response of the composite beam for each 5-minute interval, where the peak frequency response corresponds to the resonant frequency of the beam in such a time interval. By plotting all obtained power spectra side-by-side, and observing the resulting surface from above (with colours proportional to the intensity of the spectra), it is possible to

Table 2
Mix composition (see text for explanation of symbols).

Mix	Cement	c [g]	w [g]	w/c [–]	$(w/c)_v$ [–]	$c_{v\%}$ [%]	b [g]	ρ_b [g/cm^3]	w/b [–]	$(w/b)_v$ [–]	$b_{v\%}$ [%]
1	CEM I 42.5R	160.00	64.00	0.40	1.25	44.48	160.00	3.12	0.40	1.25	44.48
2	CEM I 42.5R	160.00	72.00	0.45	1.40	41.60	160.00	3.12	0.45	1.40	41.60
3	CEM I 42.5R	160.00	80.00	0.50	1.56	39.06	160.00	3.12	0.50	1.56	39.06
4	CEM I 52.5R	160.00	72.00	0.45	1.41	41.44	160.00	3.14	0.45	1.41	41.44
5	CEM II/A-L 42.5R	160.00	72.00	0.45	1.39	41.83	158.74	3.09	0.47	1.40	41.50
6	CEM II/B-L 32.5N	160.00	72.00	0.45	1.38	42.07	144.98	3.10	0.55	1.54	37.57
7	CEM II/B-L 32.5R (white)	160.00	72.00	0.45	1.34	42.72	140.82	3.02	0.58	1.55	37.10

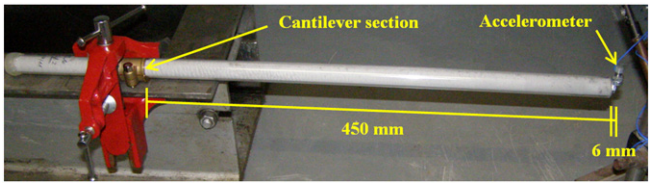

Fig. 1. Composite cantilever beam during testing.

draw the colour map shown in Fig. 2, which in turn allows tracing the evolution of the 1st resonant frequency (f) of the beam through time (t). Based on the f–t plot and the analytical equations of motion of the beam, it is possible to directly correlate the resonant frequency with the E-modulus of the tested material, thus obtaining the E–t curve, which is the final outcome of the experiment. It should be remarked that previous experiments [46] allowed observing that the levels of damping of the composite beam always remain under 5% (even at very early ages), thus allowing the simplification of considering that the damped resonant frequency is equivalent to the undamped resonant frequency (error under 0.2%) [47].

The frequency identification procedures and E-modulus estimation equations for the cement paste were implemented in a MATLAB algorithm. So, the whole set of operations is imperceptible to the final user, who receives the $E_c - t$ evolutive curve along cement hydration for each experiment directly in real-time. Nevertheless, probably owing to inaccuracies in geometry or in weight, this $E_c - t$ curve usually provides non-zero values at the beginning of the experiment (E_c lower than 0.3 GPa for all mixes). Consequently $E_c - t$ curves not starting at $E_c = 0$ GPa were shifted to satisfy such a condition at the beginning of the experiment. With regard to the resolution of E-modulus values using EMM-ARM, Maia et al. [48] reported a resolution of ± 0.02 GPa for pastes, independently of the paste maturity.

2.3. Evaluation of the E-modulus through quasi-static tests and P-wave velocity measurements

The determination of E-modulus evolution using the EMM-ARM was successfully checked by quasi-static tests (applying loading/unloading compression cycles) on concrete [22], but it lacks comparisons for pastes. In fact, there is limited information concerning the determination of the quasi-static E-modulus of cement pastes. In the present work, quasi-static tests are performed based on the experiments reported by Chamrová [5]. Summarily, samples ($40 \times 40 \times 160$ mm^3) of cement paste were made following a protocol close to the one proposed in EN196-1 [29]. Three compression cycles of loading/unloading (between 1 kN and 1/3 of the sample's compressive strength) are applied. Sample deformation is externally measured with four linear variable displacement transducers. The duration of the whole test is about 180 s (loading rate was adjusted according to the value obtained for 1/3 of compressive strength). The E-modulus was determined using the last unloading part of the last cycle.

In addition, using ultrasonic compressional waves, the velocity of the P-waves was measured along the maximum dimension of the same samples immediately after the end of each quasi-static test was finished. A 'TICO ultrasonic testing instrument' was used, having

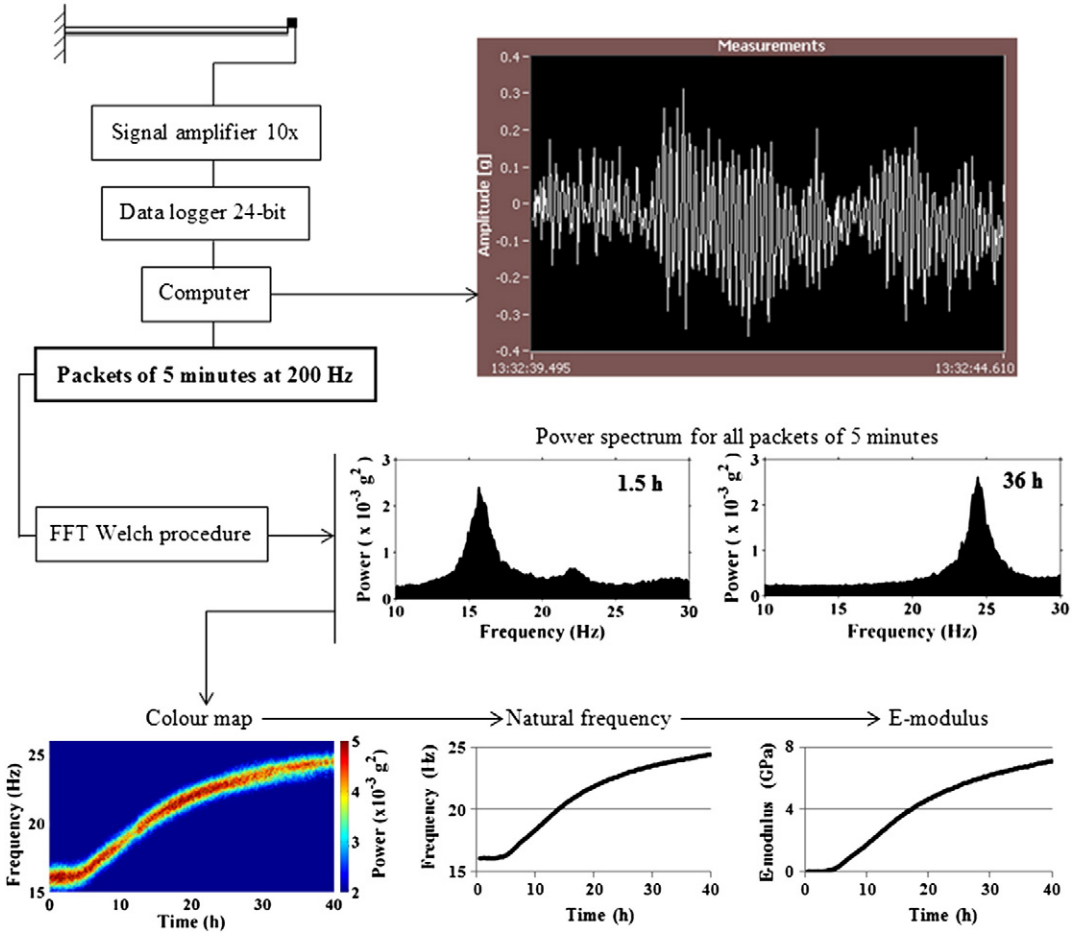

Fig. 2. Schematic set-up and data processing.

transducers with diameters of 40 mm and applying waves with 54 kHz frequency.

2.4. The percolation threshold through the percolation theory

The detection of the E-modulus initiation, which corresponds to the transition from fluid-to-solid, is important for the prediction of the E-modulus evolution. The transition from fluid-to-solid can mathematically be determined through the use of the percolation theory — a theory dealing with the degree of connectivity of disordered matter [11,49].

Assuming that at very early ages, the disordered hydrates around the cement grains initiate the development of small clusters, which start bridging with each other, thus forming larger clusters and increasing the overall degree of connectivity. This increasing connectivity eventually reaches a threshold (termed 'percolation threshold') that changes the overall behaviour of the mix from the state of a suspension of cement grains to a state of a solid material [49]. Naming p a parameter that defines the average degree of connectivity, and p_c as the percolation threshold, Gennes [50] stated that near the percolation threshold, the E-modulus E_c (and many physical properties) follows a power law:

$$E_c = E_0\,(p-p_c)^{\mu_0} \tag{3}$$

where E_0 is a constant and μ_0 is the critical exponent for the property. Considering that the number of contacts between the solids increases as a power law function of time (t) (as assumed in Ref. [51]), in the neighbourhood of the critical time (t_c), the E-modulus paste evolution can be obtained by Eq. (4):

$$E_c = E_0^{'}\,(t-t_c)^{\mu_0^{'}} \tag{4}$$

where $E_0^{'}$ and $\mu_0^{'}$ are constants. The critical time (as well as $E_0^{'}$ and $\mu_0^{'}$) can be determined by fitting Eq. (4) to the E-modulus values (for instance, obtained by the EMM-ARM) by minimizing the sum of squared residuals. However, the literature [11,16,50,51] does not clearly state what is the 'neighbourhood' of the critical time. Thus, several scenarios were studied and, as a result, the 'neighbourhood' of the critical time was defined by all the E-modulus values obtained in the range 0.10–2.0 GPa.

2.5. Hydration kinetics and degree of hydration

The degree of hydration α is defined by the ratio between the amount of cement reacted and the initial amount of cement. Although several methods have been used to measure hydration [52], none completely details the hydration process [53], nor is it possible to make continuous and direct assessments of the amount of cement that has already reacted. Therefore, when continuous measurements are required and accuracy is not crucial, indirect methods are chosen. These indirect methods are based on measuring the evolution of a property which is assumed to be proportional to the degree of hydration. Subsequently, the degree of hydration is approximated by the ratio between the value of the property P at the age t and the maximum potential value of that property P_{pot} upon complete hydration of the mineral clinker components ($\alpha = 1$) — see Eq. (5).

$$\alpha(t) = \frac{P(t)}{P_{pot}} \tag{5}$$

Considering the necessity to continuously describe the hydration process, we performed such measurements using chemical shrinkage. Chemical shrinkage is the volume reduction taking place during hydration of the cement plus water system. Even though it is directly related to the hydration reaction, one should be aware that: (i) at early ages, the chemical shrinkage evolution may be remarkably higher than the actual hydration rate due to the dissolutions [54], and (ii) for later ages, the accurate measurement of this property depends on the unhindered suction of water into the solidifying cement paste [55,56]. The maximum sample heights providing unhindered water transport during the measuring period were initially determined for the various paste compositions. In this study, the chemical shrinkage was measured by gravimetry following similar protocols used by Geiker and Knudsen [28]. The change in buoyancy of a sample with excess water on top and submerged in oil was measured. Two samples (height: 10 mm, sample diameter: 22 mm) per mix (the highest difference between samples was found to be 1.4% — thus, henceforth, average results are used) were continuously weighed from 20 min after water and cement were joined and up to the age of 168 h.

3. Results and discussion

Results of the E-modulus evolutions measured by the EMM-ARM for pastes made with commercial cements cured at 20 °C are presented and discussed in this section. However, initially the E-modulus values obtained through the EMM-ARM and quasi-static measurements are compared.

3.1. Comparison between methods to measure the E-modulus, and impact of w/c ratio and type of cement

Paste E-modulus findings previously reported in the literature, assessed either by the EMM-ARM [18,21] or ultrasonic methods [16] lack verification using quasi-static compression tests [19,57] (note that the evaluation of E-modulus in pastes by quasi-static tests is not standardized).

Initially, the relationship between the E-modulus evolution measured in prismatic samples $4\times4\times16\ cm^3$ by quasi-static tests and the corresponding P-wave velocity of the sample was checked. The pulse velocity V of the P-waves of the material is related to its elastic properties and density according to the Eq. (6).

$$V = \sqrt{\frac{E(1-\mu)}{\rho(1-\mu)(1-2\mu)}} \tag{6}$$

where μ is the dynamic Poisson's ratio, E is the dynamic modulus of elasticity, and ρ is the density [19]. Thus, assuming constant the dynamic Poisson's ratio (which is suitable due to the hydration already occurred when measurements were taken [16]), then the E-modulus vary linearly with square values of P-wave velocity.

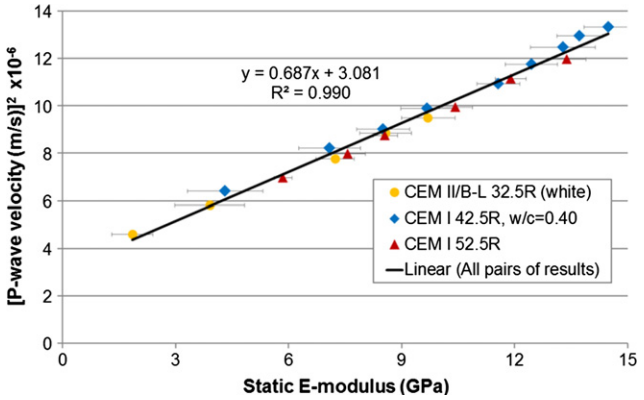

Fig. 3. Relationship between the E-modulus measured by quasi-static test and the square values of P-wave velocity of ultrasonic tests.

Fig. 3 reports the relationship between the E-modulus values obtained by quasi-static tests and the square values of P-wave velocity for the mixes made with: (i) CEM I 42.5R, w/c = 0.40; (ii) CEM I 52.5R, w/c = 0.45; and (iii) CEM II/B-L 32.5R (white), w/c = 0.45. As can be seen, it was obtained a near linear relationship between the E-modulus and square of values of the P-wave velocity (which is related to the dynamic E-modulus). Seeing that both properties follow the relationship proposed in the literature [19], one might consider that the methodology used is correctly assessing the paste E-modulus.

The E-modulus evolutions determined by the EMM-ARM are presented in Fig. 4. For comparison, the E-modulus evolutions measured by quasi-static tests are also given in Fig. 4 (note that the 'Time' for quasi-static results is expressed according to the sample temperature adjusted age to take into account maturity corrections due to the sample temperature evolution — see Section 2.1). Comparing results of the E-modulus evolution measured by different methods, one observes, that the results obtained by the quasi-static method are mostly higher (up to ~20% higher) than the results from the EMM-ARM. Seeing that the difference between the methods tends to increase at later ages, a possible explanation might be the velocity of loading during the quasi-static tests (at later ages, owing to high strength, the velocity is higher in order to complete the entire test within ~3 min — see Section 2.3). Nevertheless, even though these two methods do not provide the same values, the trend is comparable. Therefore, we consider that the EMM-ARM can be used to monitor the E-modulus evolution of cement pastes.

For pastes with lower w/c ratio, the E-modulus is higher and starts to evolve earlier than for pastes with higher w/c ratio (see Fig. 4a and Table 3). This is in agreement with the literature [7,16–18,38,41,48] and the explanation is related to the initial porosity of the pastes. Being aware that the initial volume of solids varies from 39.1% to 44.5% (see Table 2) when the w/c varies from 0.40 to 0.50, then distinct distances between solid grains require different levels of hydration to reach a specific E-modulus value.

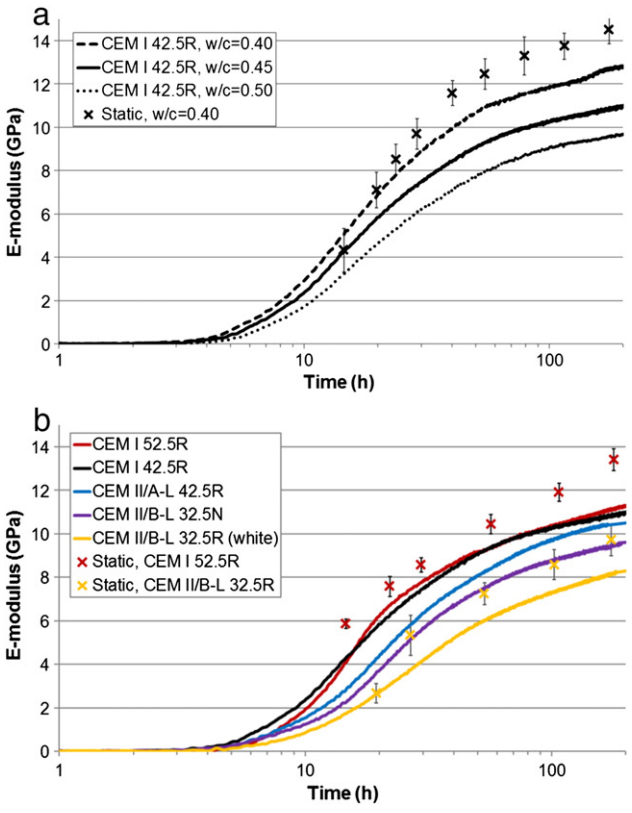

Fig. 4. E-modulus evolution (logarithmic scale) measured through the EMM-ARM and the quasi-static method for: a) pastes with distinct w/c ratios using CEM I 42.5R, and b) pastes with distinct types of cements with w/c = 0.45.

Table 3
Percolation threshold by critical time [h] and critical degree of hydration (starting from one hour).

Cement	w/c	$\dot{E_0}$	t_c	$\dot{\mu_0}$	$\sum R^2$	α_c
CEM I 52.5R	0.45	0.137	3.85	1.466	0.056	0.036
CEM I 42.5R	0.45	0.192	3.11	1.320	0.095	0.027
CEM II/A-L 42.5R	0.45	0.091	3.02	1.542	0.019	0.024
CEM II/B-L 32.5N	0.45	0.156	3.23	1.091	0.061	0.028
CEM II/B-L 32.5R (white)	0.45	0.067	3.25	1.340	0.053	0.021
CEM I 42.5R	0.40	0.221	2.80	1.323	0.049	0.026
CEM I 42.5R	0.50	0.226	3.94	1.132	0.041	0.031

For pastes from different cement types, the paste from CEM I 42.5R showed the highest early rate of E-modulus evolution (Fig. 4b). Although these pastes have quite similar initial volumes of solids per volume unit of paste (the volume of solids ranges from 41.4% to 42.7% — see Table 2), pastes showed marked different E-modulus evolutions (the reason of the difference will be discussed in detail afterwards in the Section 3.5).

3.2. Hydration kinetics by chemical shrinkage evolution

The hydration evolutions measured as chemical shrinkage development are given in Fig. 5 for all the studied mixes. The results are later used to determine the degree of hydration (after being divided by the corresponding V_{pot}, as referred in Section 2.5).

Due to time needed for mixing, casting and temperature equilibrium [28], measurements were zeroed at the age of 1.0 h (likewise for several other authors [16,41,58,59]). As C–S–H is the most vital hydration product for cohesion and enhancement of mechanical properties [5], and mostly dissolution takes place during the first hour after mixing [53], it is considered acceptable to neglect the first hour of chemical shrinkage results.

From Fig. 5, one can generally infer that the chemical shrinkage variation between mixes is related to the amount of reacting binder in the different cements. For mixes with CEM I 42.5R varying in w/c ratios, it can be observed that at later ages the chemical shrinkage is lower for the mix with w/c = 0.40. According to Geiker [55] this may be due to lack of pore connectivity in the mix with the lowest w/c ratio, but space limitations may be also the reason.

3.3. Percolation threshold

The evolution of resonant frequency measured by EMM-ARM and the hydration kinetics measured as chemical shrinkage rate are presented in Fig. 6. The figure covers data up to the age of 12 h for pastes

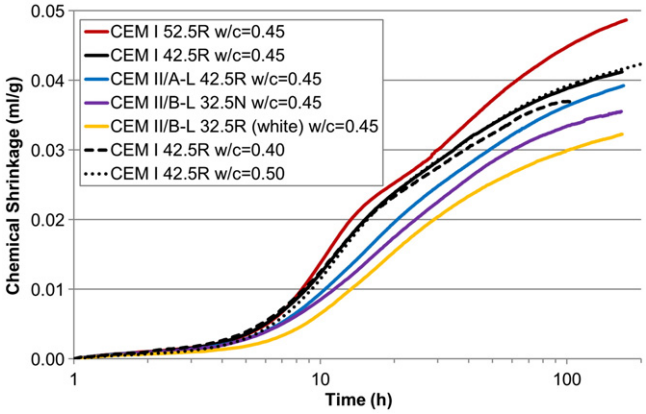

Fig. 5. Chemical shrinkage evolution per gram of cement (logarithmic scale).

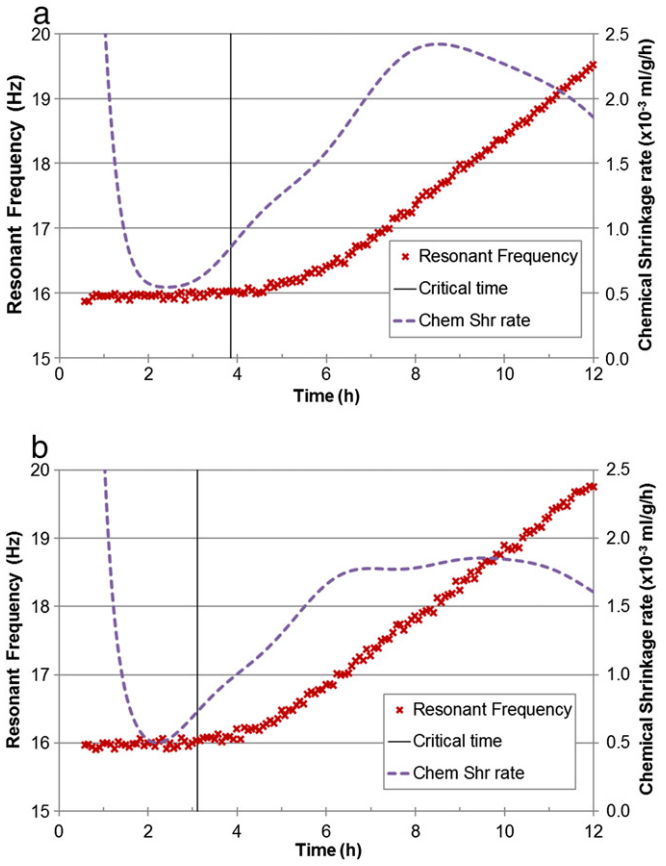

Fig. 6. Evolution of the resonant frequency with the hydration rate assessed by chemical shrinkage for cement pastes with w/c = 0.45 performed with: a) CEM I 52.5R and b) CEM I 42.5R.

made from the cements type I with w/c = 0.45 (CEM I 52.5R in Fig. 6a and CEM I 42.5R in Fig. 6b). In addition, vertical lines corresponding to the critical times — determined by adjusting a power law (Eq. (4) — see Section 2.4) — are presented. Note that the critical times are located when the natural frequency starts to increase (it corresponds to the moment wherein the E-modulus starts to rise from zero). Similar findings were also observed for the other pastes studied. The values of the critical times (as well as $E_0^{'}$ and $\mu_0^{'}$) obtained through application of Eq. (4) are represented in Table 3 for all the pastes under study.

Seeing that all the critical times, calculated using Eq. (4), were found to be close to the ages at which the E-moduli start developing, one can then conclude that the critical time defined by the percolation theory is appropriate to identify the transition from fluid-to-solid — the percolation threshold. Supporting the previous conclusion is also the slight difference (which was always lower than 2 h for all mixes) between the beginning of the hydration accelerating period (observable from the chemical shrinkage rate) and the location of the critical time observed in Fig. 6. Similar differences were also noticed by other authors who compared hydration rates with results from ultrasonic [20] or rheometric [33] methods.

Such differences are observable because the E-modulus starts to evolve only after a certain degree of hydration is reached (critical degree of hydration — α_c). Before the percolation threshold occurred the solids are not connected. Some initial hydration must have taken place to connect the solids [20,56]. Table 3 indicates that for the investigated pastes, α_c varies from about 0.021 to 0.036. Information available in the literature is not consistent with regard to α_c values; partly due to variation of the time of beginning measurements of hydration [5]. Our findings of α_c fall within the range of previously reported values by authors who zeroed the degree of hydration at the age of 1 h: (i) Boumiz [16] reported $\alpha_c = 0.0208$ and 0.0261 for C_3S pastes, and $\alpha_c = 0.0294$ and 0.0392 for white cement pastes with w/c = 0.40 and 0.50, respectively; (ii) using oil well cement, Zhang et al. [41] reported a linear relationship between the α_c and w/c: being reported $\alpha_c \sim 0.043$ when w/c = 0.40.

3.4. E-modulus evolution as a function of the degree of hydration

Like other mechanical properties, the E-modulus evolution is usually presented as a function of the degree of hydration. Thus, the E-moduli evolutions reported in Fig. 4 are displayed in Fig. 7 as a function of the degree of hydration — which is determined by dividing the measured chemical shrinkage (Fig. 5) by the estimated total chemical shrinkage, V_{pot} (Table 1). Looking at Fig. 7 one observes that the E-modulus evolves approximately linearly with the degree of hydration in the range from approximately 0.05 to 0.3. This is consistent with the tendencies found between ultrasonic reflection loss and calorimetry, chemical shrinkage or non-evaporable water reported in Refs. [39,40]. For higher degrees of hydration changes in the slope and/or non-linearity are observed, especially for CEM I 52.5R.

In Fig. 7a findings reported by Boumiz [16] for pastes of C_3S and white cement are also presented. It can be observed that the E-modulus evolutions obtained by EMM-ARM are much lower than the findings reported by Boumiz [16] (see Fig. 7a). Boumiz's results for white cement paste are, roughly speaking, two times larger than the E-modulus measured in the present study for CEM I 42.5R; part of which can be explained by the hydration products having a larger specific volume and a different morphology. Up to the degree of hydration of ~0.25 our findings are somewhat closer to Boumiz's for C_3S pastes, but for higher degrees of hydration, even the C_3S pastes show higher E-moduli than those measured in the present study.

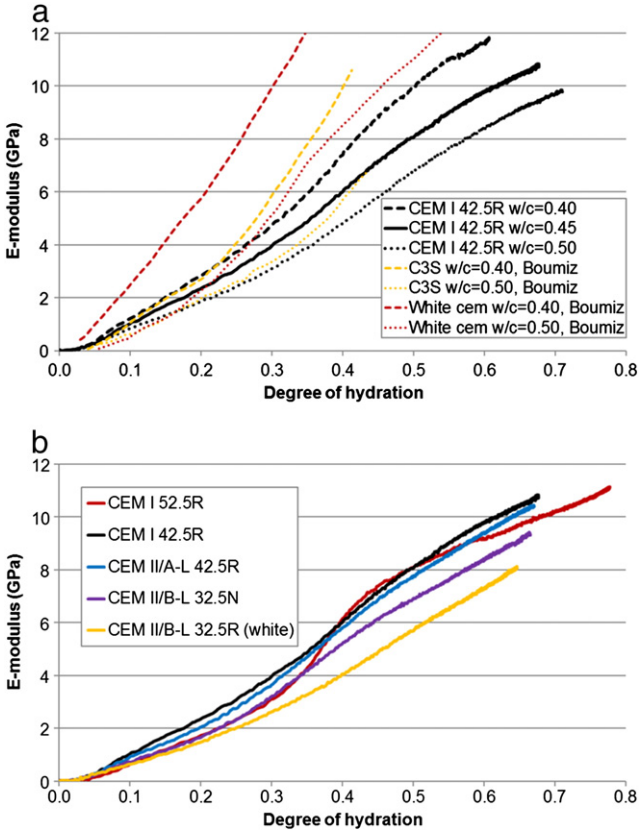

Fig. 7. a) E-modulus evolution as a function of the degree of hydration for: a) cement pastes with varying w/c ratios, and b) cement pastes from varying cement types with w/c = 0.45.

The difference previously reported in Section 3.1 between findings obtained through the EMM-ARM and the quasi-static ones can only explain ~20%. The main difference between findings might be explained by the fact that Boumiz [16] has used ultrasonic techniques. Consequently, Boumiz [16] was probably measuring a property much related to the dynamic E-modulus [19], which can be quite a bit higher than the quasi-static ones, as can be observed in Ref. [5]. Unfortunately, the lack of data in the literature, does not allow us to go further into this discussion.

3.5. The influence of the limestone filler

In Figs. 4b and 7b, it is possible to observe that pastes with similar initial volume of cement exhibit different E-moduli evolutions. We think that the key feature to explain the distinct E-moduli evolutions observed may be the limestone filler content included in the different commercial cements, although other factors (such as, fineness and mineral composition of the clinker) might also have some influence. Note that, when a specific volume of clinker is replaced by the same volume of limestone filler, the total volume of solids remains unchanged but the water-to-clinker ratio is increased.

According to Lothenbach et al. [23], limestone filler enhances the formation of monocarbonate. Consequently, it indirectly induces a stabilization of the ettringite (instead of being consumed into monosulfate) which leads to an increase in the total volume of the solid phases and a decreased porosity. In addition, when the limestone is finely ground, it provides additional surfaces for nucleation of hydration products, thus shortening the dormant period and enhancing the hydration kinetics [60,61]. However, if the limestone filler content exceeds approximately 5% (it depends on the alumina content) of the cement, dilution effects of the clinker become dominant [23].

Comparing the E-modulus evolution, shown in Fig. 4b, for the pastes made with cements CEM I 52.5R and CEM I 42.5R (no limestone filler and with all the limestone filler being considered as binder, respectively, having the initial volume of solids quite similar — 41.4% and 41.6%, respectively) it is noticeable that the presence of limestone filler seems to affect the E-modulus evolution. The paste with CEM I 42.5R (the coarser cement, containing 4.5% of limestone filler), reaches the percolation threshold earlier and presents the highest E-modulus up to the age of ~15 h. A possible explanation is that nucleation and growth control the early hydration kinetics, and changing clinker grains for limestone filler grains causes the water available per gram of clinker to increase without a decrease in the nucleation sites [62].

For the other cements in which part of the limestone filler is considered inert, comparisons are more difficult because the initial volume of solids is quite a bit different (see Table 2). Roughly speaking, a decrease in volume of (reactive) binder in the mix tends to slow down the E-modulus evolution (see Figs. 4b and 7b).

3.6. Relationship between the E-modulus and chemical shrinkage evolutions

Being aware that the E-modulus evolution is related to the volume of connected solid grains, it is relevant to correlate results of the E-modulus evolution to the formation of solid products. It was referred in Section 2.5 that chemical shrinkage is an indirect method to monitor the hydration reaction. Assuming comparable reactants and products, one can assume that for the same value measured of chemical shrinkage the same amount of solids has formed. Note that, the degree of hydration is a property that quantifies the relative amount of binder reacted (see Eq. (5)), whereas, chemical shrinkage is a measure of the absolute amount of binder reacted.

The E-modulus evolution is plotted against chemical shrinkage (per volume unit of paste) in Fig. 8. In this figure, it can be inferred that pastes with similar volume of cement per volume unit present quite similar E-modulus for the same chemical shrinkage (compare to Fig. 7b, where the degree of hydration is used). Consequently, and bearing in mind that pastes with the same w/c ratio have comparable initial volume of solids (due to slight differences in the cement specific mass, volume of solids varies from 41.4% to 42.7%), one may conclude that for the same initial volume of solids the E-modulus evolution is not related to the degree of hydration, but to the amount of solids formed.

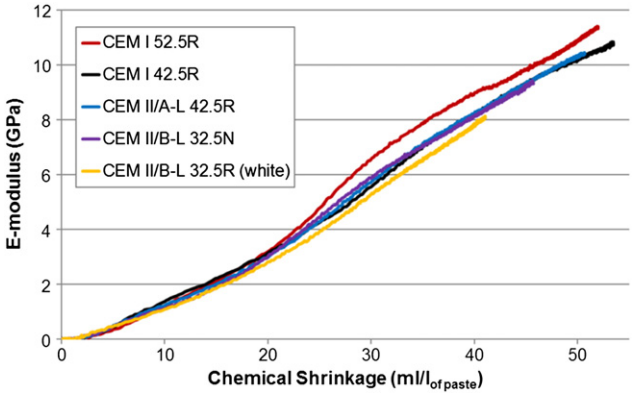

Fig. 8. E-modulus evolution vs. chemical shrinkage evolution (per volume unit).

Present prediction models for E-modulus evolution [5–11] may not be completely appropriate for pastes made from commercial cements, and thus may be object of improvement. A feasible step towards developing models to predict the E-modulus of pastes from commercial cements could be to describe the E-modulus evolution as a function of a property directly related to the volume of solids formed, instead of the degree of hydration of the cement.

4. Conclusions

From the results presented in this paper the following conclusions can be drawn:

- The EMM-ARM seems a feasible method for the continuous measurement of E-modulus evolution of cement pastes. The results obtained were slightly lower than the ones obtained through a quasi-static method.
- The EMM-ARM appears to have enough sensitivity to detect the percolation threshold.
- The E-modulus evolution is related to the formation of solids. Therefore, it is strongly influenced by the water-to-cement ratio, which rules the initial solid volume, and the degree of reaction.
- For the investigated cement pastes with the same water-to-cement ratio, the E-modulus evolution was related to the chemical shrinkage development (which is an indirect measure of the solid formation).
- Limestone filler enhances the hydration kinetics and thus the rate of solid formation. Limestone in excess of approximately 5% reduced the E-modulus evolution. The impact of unreactive filler in the cement on the E-modulus evolution may be taken into account using a corrected w/b ratio.

Based on the above, it is suggested that for commercial cements it could be more appropriate to model the E-modulus evolution based on the amount of binder reacted, instead of the degree of hydration.

Acknowledgments

Funding provided by the Portuguese Foundation for Science and Technology (FCT) and the European Social Fund (ESF), namely to the Research Projects PTDC/ECM/70693/2006 and PTDC/ECM/099250/2008, and to the first author through the PhD grant SFRH/BD/24427/2005, is gratefully acknowledged. Also, the first author would like thank the

Department of Civil Engineering, Technical University of Denmark for hosting him during three research visits.

References

[1] RILEM TC 181-EAS, Early Age Cracking in Cementitious Systems — Report of RILEM Technical Committee 181-EAS — Early Age Shrinkage Induced Stresses and Cracking in Cementitious Systems, RILEM Publications SARL, 2003.
[2] RILEM TC 119-TCE, Prevention of thermal cracking in concrete at early ages — recommendations of TC 119-TCE — avoidance of thermal cracking in concrete at early ages E& FN Spon, 1998.
[3] ACI 231R-10, Report on early-age cracking: causes, measurement, and mitigation, Reported by ACI Committee 231, ACI, 2010.
[4] F. Rostásy, A. Gutsch, M. Krauß, Computation of stresses and cracking criteria for early age concrete — methods of iBMB, IPACS, 2001.
[5] R. Chamrová, Modelling and measurement of elastic properties of hydrating cement paste, À La Faculté Sciences Et Techniques De L'ingénieur, École Polytechnique Fédérale De Lausanne, 2010.
[6] L. Stefan, F. Benboudjema, J.-M. Torrenti, B. Bissonnette, Prediction of elastic properties of cement pastes at early ages, Comput. Mater. Sci. 47 (2010) 775–784.
[7] C.J. Haecker, E.J. Garboczi, J.W. Bullard, R.B. Bohn, Z. Sun, S.P. Shah, T. Voigt, Modeling the linear elastic properties of Portland cement paste, Cem. Concr. Res. 35 (2005) 1948–1960.
[8] Y. Qing-Sheng, L. Chun-Jiang, Evolution of properties in hydration of cements — a numerical study, Mech. Res. Commun. 33 (2006) 717–727.
[9] O. Bernard, F.-J. Ulm, E. Lemarchand, A multiscale micromechanics — hydration model for the early-age elastic properties of cement-based materials, Cem. Concr. Res. 33 (2003) 1293–1309.
[10] J. Sanahuja, L. Dormieux, G. Chanvillard, Modelling elasticity of a hydrating cement paste, Cem. Concr. Res. 37 (2007) 1427–1439.
[11] V. Smilauer, Z. Bittnar, Microstructure-based micromechanical prediction of elastic properties in hydrating cement paste, Cem. Concr. Res. 36 (2006) 1708–1718.
[12] D.P. Bentz, CEMHYD3D: a Three-Dimensional Cement Hydration and Microstructure Development Modelling Package. Version 2.0, NISTIR 6485, US Department of Commerce, 2000.
[13] G. Constantinides, F.-J. Ulm, The effect of two types of C–S–H on the elasticity of cement-based materials: results from nanoindentation and micromechanical modeling, Cem. Concr. Res. 34 (2004) 67–80.
[14] K. Velez, S. Maximilien, D. Damidot, G. Fantozzi, F. Sorrentino, Determination by nanoindentation of elastic modulus and hardness of pure constituents of Portland cement clinker, Cem. Concr. Res. 31 (2001) 555–561.
[15] P. Lura, P. Trtik, B. Münch, Validity of recent approaches for statistical nanoindentation of cement pastes, Cem. Concr. Compos. 33 (2011) 457–465.
[16] A. Boumiz, Etude comparée des évolutions mécaniques et chimiques des pâtes de ciment et mortiers a très jeune age. Développement des techniques acoustiques, in: Acoustique Physique, Thèse de Doctorat de l'Université Paris 7, 1995.
[17] Z. Sun, T. Voigt, S.P. Shah, Rheometric and ultrasonic investigations of viscoelastic properties of fresh Portland cement pastes, Cem. Concr. Res. 36 (2006) 278–287.
[18] L. Maia, M. Azenha, R. Faria, J. Figueiras, Influence of the cementitious paste composition on the E-modulus and heat of hydration evolutions, Cem. Concr. Res. 41 (2011) 799–807.
[19] ASTM C 597 - 97, Standard Test Method for Pulse Velocity through Concrete, American Society for Testing and Materials, Philadelphia, PA, 1997 1998.
[20] G. Sant, M. Dehadrai, D. Bentz, P. Lura, C.F. Ferraris, J.W. Bullard, J. Weiss, Detecting the fluid-to-solid transition in cement pastes, Concr. Int. 31 (2009) 53–58.
[21] M. Azenha, R. Faria, F. Magalhães, L. Ramos, Á. Cunha, Measurement of the E-modulus of cement pastes and mortars since casting, using a vibration based technique, Mater. Struct. (2011) 1–12.
[22] M. Azenha, F. Magalhães, R. Faria, Á. Cunha, Measurement of concrete E-modulus evolution since casting: a novel method based on ambient vibration, Cem. Concr. Res. 40 (2010) 1096–1105.
[23] B. Lothenbach, G. Le Saout, E. Gallucci, K. Scrivener, Influence of limestone on the hydration of Portland cements, Cem. Concr. Res. 38 (2008) 848–860.
[24] EN 197–1:2000 - Cement - Part 1: Composition, specifications and conformity criteria for common cements, 2000.
[25] H.F.W. Taylor, Cement Chemistry, Academic Press, 1990.
[26] D. Bentz, Exercise, Bogue Calculations and Property Predictions, Summer School, DTU, 1999.
[27] L. Maia, M.R. Geiker, J.A. Figueiras, Hydration of Portuguese cements, measurement and modelling of chemical shrinkage, in: L.J.A. Marques, A. Henriques, R. Faria, J. Barros, A. Ferreira (Eds.), CCC2008: Challenges for Civil Construction, Faculty of Engineering of the University of Porto, Porto, Portugal, 2008, p. 12.
[28] M. Geiker, T. Knudsen, Chemical shrinkage of Portland cement pastes, Cem. Concr. Res. 12 (1982) 603–610.
[29] EN 196-1:2005 (European Norm), Methods of Testing Cement, Part 1: Determination of Strength, 2005.
[30] EN 1992-1-1:2004, Eurocode 2: Design of Concrete Structures — Part 1-1: General Rules and Rules for Buildings, 2004.
[31] ASTM C 469, Standard Test Method for Static Modulus of Elasticity and Poisson's Ratio of Concrete in Compression, American Society for Testing and Materials, Philadelphia, PA, 2002.
[32] ISO 1920-10:2010, Testing of Concrete Part 10: Determination of Static Modulus of Elasticity in Compression, 2010.
[33] G. Sant, C.F. Ferraris, J. Weiss, Rheological properties of cement pastes: a discussion of structure formation and mechanical property development, Cem. Concr. Res. 38 (2008) 1286–1296.
[34] K.V. Subramaniam, X. Wang, An investigation of microstructure evolution in cement paste through setting using ultrasonic and rheological measurements, Cem. Concr. Res. 40 (2010) 33–44.
[35] S.P. Pessiki, N.J. Carino, Setting time and strength of concrete using the impact-echo method, ACI Mater. J. 85 (1988) 389–399.
[36] M. Krauß, K. Hariri, Determination of initial degree of hydration for improvement of early-age properties of concrete using ultrasonic wave propagation, Cem. Concr. Compos. 28 (2006) 299–306.
[37] H.W. Reinhardt, C.U. Grosse, Continuous monitoring of setting and hardening of mortar and concrete, Constr. Build. Mater. 18 (2004) 145–154.
[38] M.I. Valic, Hydration of cementitious materials by pulse echo USWR: method, apparatus and application examples, Cem. Concr. Res. 30 (2000) 1633–1640.
[39] T. Voigt, C. Grosse, Z. Sun, S. Shah, H. Reinhardt, Comparison of ultrasonic wave transmission and reflection measurements with P- and S-waves on early age mortar and concrete, Mater. Struct. 38 (2005) 729–738.
[40] T. Voigt, G. Ye, Z. Sun, S.P. Shah, K. van Breugel, Early age microstructure of Portland cement mortar investigated by ultrasonic shear waves and numerical simulation, Cem. Concr. Res. 35 (2005) 858–866.
[41] J. Zhang, E.A. Weissinger, S. Peethamparan, G.W. Scherer, Early hydration and setting of oil well cement, Cem. Concr. Res. 40 (2010) 1023–1033.
[42] ASTM C 215, Standard Test Method for Fundamental Transverse, Longitudinal, and Torsional Resonant Frequencies of Concrete Specimens, American Society for Testing and Materials, Philadelphia, PA, 2002.
[43] J. Granja, Evolution of E-modulus of cementitious materials since early ages: experimental assessment and numerical simulation (in Portuguese), in: MSc Thesis, Engineering School, University of Minho, Guimarães, 2011.
[44] M. Azenha, Numerical Simulation of the Structural Behaviour of Concrete since its Early Ages, Faculty of Engineering - University of Porto, Porto, 2009, p. 375.
[45] P. Welch, The use of fast Fourier transform for the estimation of power spectra: a method based on time averaging over short modified periodograms, IEEE Trans. Audio Electroacoust. 15 (2) (1967).
[46] R.A. Velez, Dynamic structural identification using Wireless Sensor Networks, in: PhD Thesis, Engineering School, University of Minho, Guimarães, 2010, pp. 225.
[47] A.K. Chopra, Dynamics of Structures: Theory and Applications to Earthquake Engineering, Third ed. Prentice Hall, 2006.
[48] L. Maia, M. Azenha, R. Faria, J. Figueiras, Identification of the percolation threshold in cementitious pastes by monitoring the E-modulus evolution, Cement and Concrete Composites 34 (2012) 739–745.
[49] D.P. Bentz, E.J. Garboczi, Percolation of phases in a three-dimensional cement paste microstructural model, Cem. Concr. Res. 21 (1991) 325–344.
[50] P.-G. de Gennes, On a relation between percolation theory and the elasticity of gels, J. Phys. Lett. 37 (1976) L1–L2.
[51] B. Gauthier-Manuel, E. Guyon, Critical elasticity of polyacrylamide above its gel point, J. Phys. Lett. 41 (1980) L503–L505.
[52] K.v. Breugel, Simulation of Hydration and Formation of Structure in Hardening Cement-based Materials, Second ed. Delft University Press, 1997.
[53] J.W. Bullard, H.M. Jennings, R.A. Livingston, A. Nonat, G.W. Scherer, J.S. Schweitzer, K.L. Scrivener, J.J. Thomas, Mechanisms of cement hydration, Cem. Concr. Res. 41 (2011) 1208–1223.
[54] M. Buil, Studies of the shrinkage of hardening cement paste (in French), Rapport de recherche LPC No 92, Laboratoire Central des Ponts et Chaussées, Paris, 1979.
[55] M. Geiker, Studies of Portland cement hydration by measurements of chemical shrinkage and systematic evaluation of hydration curves by means of the dispersion model, Institut of Mineral Industry, Technical University of Denmark, Lyngby, 1983.
[56] M. Dehadrai, G. Sant, D. Bentz, J. Weiss, Identifying the fluid-to-solid transition in cementitious materials at early ages using ultrasonic wave velocity and computer simulation, Concr. Int. 259 (2009) 66–76.
[57] T. Voigt, The Application of an Ultrasonic Shear Wave Reflection Method for Nondestructive Testing of Cement-Based Materials at Early Ages: An Experimental and Numerical Analysis, in, University of Leipzig, Germany, Books on Demand, Norderstedt, 2005, pp. 244.
[58] P. Mounanga, A. Khelidj, A. Loukili, V. Baroghel-Bouny, Predicting Ca(OH)2 content and chemical shrinkage of hydrating cement pastes using analytical approach, Cem. Concr. Res. 34 (2004) 255–265.
[59] L.J. Parrott, M. Geiker, W.A. Gutteridge, D. Killoh, Monitoring Portland cement hydration: comparison of methods, Cem. Concr. Res. (1990) 919–926.
[60] A.-M. Poppe, G. De Schutter, Cement hydration in the presence of high filler contents, Cem. Concr. Res. 35 (2005) 2290–2299.
[61] D.P. Bentz, Modeling the influence of limestone filler on cement hydration using CEMHYD3D, Cem. Concr. Compos. 28 (2006) 124–129.
[62] B. Lothenbach, K. Scrivener, R.D. Hooton, Supplementary cementitious materials, Cem. Concr. Res. 41 (2011) 217–229.